

ARTICLES

Tunneling solutions of the Hamilton-Jacobi equation for multidimensional semiclassical theory

Kazuo Takatsuka and Hiroshi Ushiyama

Graduate School of Human Informatics, Nagoya University, Nagoya 464-01, Japan

(Received 19 April 1994)

A class of complex solutions to the time-independent Hamilton-Jacobi equation in the real-valued configuration space that represent multidimensional nonclassical motions such as dynamical tunneling, namely, energetically allowed but dynamically forbidden transition, as well as the ordinary tunneling are shown. We introduce a quantity called "parity of motion" into each coordinate in configuration space for the Hamilton-Jacobi equation and thereby construct the solutions. Positive parity induces merely ordinary classical motion, while negative parity allows nonclassical motion such as tunneling. These solutions are classified by a given set of parities, each class of which forms a sheet in the entire solution space. New canonical equations of motion are derived with which nonclassical paths are generated in each sheet. Furthermore, it is shown that each sheet is associated with two kinds of action integrals: One, which is real valued, satisfies the principle of least action, thereby generating both ordinary and tunneling trajectories, but is not a solution to the Hamilton-Jacobi equation, while the other action is a solution to the time-independent Hamilton-Jacobi equation, and is complex valued in a tunneling region. Only in Newtonian mechanics, which forms an extreme sheet having all the parities positive, do these two actions happen to coincide with each other. Numerical examples for dynamical tunneling among tori in the Hénon-Heiles system and ordinary potential tunneling in a three-dimensional system are presented.

PACS number(s): 03.65.Sq, 73.40.Gk, 05.45.+b

I. INTRODUCTION

The tunneling effect is one of the most fundamental concepts that only quantum mechanics has revealed [1,2]. Many phenomena related to tunneling are widely observed and applied in many areas of microscopic science and technology. Nevertheless, the understanding of this phenomenon to date does not seem complete yet. This is mostly because the tunnel effect is usually discerned based on classical concepts such as the energy of a classical path. This fact suggests, on the other hand, that new insights in classical mechanics, such as Hamilton chaos [3], can renew the current interest in the tunnel effect. In return, the definition of tunneling can become more and more vague depending on how classical mechanics is extended. Here, in the present paper, the word tunneling is used almost as a synonym of "nonclassical motion." In particular, we are not confined to the usual tunneling (called potential tunneling) in which the total energy of a path is lower than a potential. Rather, our attention is paid more to tunneling (dynamical tunneling) that connects energetically accessible but dynamically separated classical paths.

The study of classical chaos has made great progress during the last three decades [3], although the importance of nonintegrability has long been recognized since the age of Poincaré. The stability of the orbits of the planets and classical ergodicity as a theoretical foundation of statistical mechanics are among the subjects under strong focus [4]. Semiclassical studies on the mechanism of quantization of classical chaos are also one of the most exciting problems in fundamental science [5,6], since the Einstein-Brillouin-Keller (EBK) conditions [7], or torus

quantization, is not relevant to nonintegrable (chaotic) systems. The role of tunneling in chaos is another very interesting subject, since the infinite valuedness of a chaotic solution of the Hamilton-Jacobi equation can give birth to infinitely many caustics almost everywhere [8], from each of which tunneling could take place.

We address, in the present and succeeding presentations, the problem of tunneling and geometry of caustics in a weakly chaotic system. By weak chaos, we mean a situation in which relatively *thin* quasiseparatrices [3(a)], or a chaotic zone, coexist with tori that are surrounded by the separatrices in phase space. In molecular vibration as an example, different tori separated geometrically by a quasiseparatrix give rise to qualitatively different vibrational modes. On the other hand, trajectories in the quasiseparatrix undergo these possible modes alternately with an unpredictable sequence of transitions [9]. This very curious behavior extends the concept of the so-called large-amplitude motion in molecular vibration. The quantum version of this weak chaos has also been studied in our laboratory [10].

Here, we concentrate on tunneling from one torus to another. In order to treat this problem and the usual potential tunneling as well, an appropriate multidimensional semiclassical theory [11] is necessary. For the one-dimensional case, in which dynamical tunneling has no way to appear, semiclassical theory for tunneling has been well established [12]. In a multidimensional case, it is quite well known that the so-called instanton path is considered naturally in the framework of path integrals [11b,13]. In particular, the method of path decomposition expansion [13] has led to a deep understanding of multidimensional tunneling, although no dynamical tun-

neling has been treated. Generating the instanton paths is particularly simple, because they are required to run "classically" on a reversed potential. Recently, Huang, Feuchtwang, Culter, and Kaze [1] have devised an innovative method based on the Huygens principle to propagate "global" solutions of the time-independent Hamilton-Jacobi equation in the tunneling region. Both tunneling paths and the action integral are calculated simultaneously in a kind of iterative manner. Takada and Nakamura [2] have made major progress in this line: They have settled the connection problem among the solutions in different branches, and actually carried out numerical calculations of the method of Huang *et al.* in two-dimensional systems and thereby found a new class of global solution. Since their works are relevant to our study, they will be referred to later.

In the present paper, we will show that the time-independent Hamilton-Jacobi equation [14] has a class of complex-valued "local" solutions in real configuration space, namely, a complex action integral along a different kind of real-valued trajectory. This is accomplished by introducing "parity of motion" that takes direct advantage of the property inherent in the Hamilton-Jacobi equation. A parity, which can be either 1 or -1 , is assigned to each coordinate. It is shown that a given set of parities gives rise to its own canonical equations of motion. The entire set of trajectories thus generated by all the possible combinations of the parities forms a layer structure composed of many sheets, each of which is characterized in terms of a parity set. (The sheet here means essentially a branch of solutions. However, the word branch is reserved for the usual sense in the Hamilton-Jacobi theory and the WKB approximation [11]. A single sheet therefore can have many branches.) For the parity of 1, motion in this coordinate is essentially the same as that of Newtonian mechanics. On the other hand, motion in a direction to which the parity of -1 is assigned tends to climb a potential slope against the force applied. In this way, classical mechanics can be extended beyond the ordinary Newton mechanics. However, the "nonclassical" solutions are of physical relevance only when considered in the context of quantum (or semiclassical) mechanics. For instance, tunneling is regarded as a sequence of paths that starts in the ordinary space (sheet) with all the positive parities, and jumps into one of nonclassical sheets at some caustic point and stays there for a short "time," then comes back to the original space. Furthermore, it is shown that two different action integrals are associated with each sheet. One is real valued, and satisfies the principle of least action and thereby generates nonclassical (tunneling) paths, but is not a solution to the Hamilton-Jacobi equation. The other is a complex-valued solution to the time-independent Hamilton-Jacobi equation. Both these action integrals and geometries of paths should be connected smoothly with those of the neighboring sheets, respectively. We thus find local but nonclassical solutions to the Hamilton-Jacobi equation. One of the greatest advantages of constructing the local solution is, of course, its applicability to many-dimensional systems.

The solution space includes two extreme sheets. One is

that for the Newtonian mechanics as stated above, and the other is that for the so-called instanton paths [11(b),13] for which all the parities are negative. Our theory claims with explicit construction that in between these extremes there exist many independent solutions.

The structure of the present paper is as follows. In Sec. II, we extend classical mechanics so that nonclassical paths can be generated. The action integral which is a solution of the time-independent Hamilton-Jacobi equation is constructed in Sec. III. Some numerical examples for various tunnelings, including dynamical tunneling among different tori, are presented in Sec. IV. The paper concludes in Sec. V with some remarks.

II. PARITY OF MOTION

A. The stationary-state Hamilton-Jacobi equation

Our goal in the present paper is to find local and nonclassical solutions in the time-independent Hamilton-Jacobi (HJ) equation [14] for a given energy E ,

$$\frac{1}{2} \sum_k \left[\frac{\partial W}{\partial q_k} \right]^2 + V(\vec{q}) = E, \quad (2.1)$$

where V is a potential energy in configuration space $\{q_i, i=1, \dots, N\}$. We use the so-called mass-weighted coordinates so that all the masses that otherwise should have been included in Eq. (2.1) can be taken to be unity. The HJ equation corresponds to the standard classical Hamiltonian

$$H = \sum_k \frac{1}{2} p_k^2 + V(\vec{q}). \quad (2.2)$$

The solutions of the HJ equation are vital to quantum mechanics as well, since as is well known the HJ equation can be found as the lowest-order approximation to the WKB expansion of the Schrödinger equation [11,12]. However, it has been suggested by Schrödinger himself that the HJ equation is more than equivalent to Newtonian (or Hamiltonian) mechanics. This can be seen clearly by a transformation [15]

$$W = K \ln \psi, \quad (2.3)$$

which leads to

$$\frac{K^2}{2} \sum_k \left[\frac{\partial \psi}{\partial q_k} \right]^2 + [V(\vec{q}) - E] \psi^2 = 0. \quad (2.4)$$

Then the variational functional

$$I(\psi, \psi') = \int f(\psi(\vec{q}), \psi'(\vec{q})) d\vec{q} \quad (2.5)$$

with

$$f(\psi, \psi') = \frac{K^2}{2} \sum_k \left[\frac{\partial \psi}{\partial q_k} \right]^2 + [V(\vec{q}) - E] \psi^2 \quad (2.6)$$

is made stationary, where ψ' is a collective representation of the first derivatives of ψ with respect to all q_k 's. The Euler-Lagrange variational procedure under appropriate boundary conditions gives the stationary-state

Schrödinger equation

$$-\frac{K^2}{2} \sum_k \frac{\partial^2 \psi}{\partial q_k^2} + V(\vec{q})\psi = E\psi \quad (2.7)$$

with the replacement $K = \hbar$. This derivation suggests that solutions to the Schrödinger equation could be constructed in terms of the general solutions, including non-classical ones, of the HJ equation. (We are not claiming that the HJ equation is equivalent to the Schrödinger equation.)

In pure classical (Newtonian) mechanics, it is sufficient to consider only the real-valued solutions in a real configuration space. However, the most important point in the above quantum-classical correspondence is the relation of Eq. (2.3), where a wave function can be either positive or negative, or even complex in this space. Accordingly, the function W in this situation should be generally complex in real space. In fact, Takada and Nakamura [2] are probably the first who actually constructed not only pure imaginary but also complex global solutions to the HJ equation in two-dimensional systems. They solved the Huygens principle of Huang *et al.* [1] numerically in a tunneling region. A non-pure-imaginary complex solution is important because it gives a new kind of tunneling that had not been considered before (see Ref. [2] and our later discussion). We thus remain in the real-valued configuration space rather than making analytical continuation into a multidimensional complex space, which is a standard, but never simple, idea in the sophisticated versions of semiclassical theory [11(a),12,16–18].

On the other hand, one of the greatest virtues of the HJ equation is that it gives local solutions such as classical trajectories through the canonical equations of motion [14]. A really multidimensional problem, of more than two degrees of freedom, can be solved because a solution is propagated along a trajectory. This idea always lies behind any semiclassical theory, even for a tunneling problem. We therefore attempt to propagate a local complex solution of the HJ equation along a path that is newly constructed in real-valued configuration space.

B. Parity of motion

Upon looking at the HJ equation, Eq. (2.1), we immediately notice that it is invariant to multiplying the following constant σ_k for each coordinate k such that

$$\frac{1}{2} \sum_k \left[\frac{1}{\sigma_k} \frac{\partial W}{\partial q_k} \right]^2 + V(\vec{q}) = \frac{1}{2} \sum_k \left[\frac{\partial W}{\partial q_k} \right]^2 + V(\vec{q}) = E, \quad (2.8)$$

provided that $\sigma_k^2 = 1$. We call this constant “parity of motion,” since it is simply 1 or -1 . The effect of the parities is not as trivial as it seems at first sight. Rewrite the HJ equation as

$$\frac{1}{2} \sum_k (\dot{q}_k)^2 + V(\vec{q}) = \frac{1}{2} \sum_k \left[\frac{\partial L_{\text{cl}}}{\partial \dot{q}_k} \right]^2 + V(\vec{q}) = E, \quad (2.9)$$

with use of the standard relation between the classical Lagrangian L_{cl} and W [14]

$$\frac{\partial L_{\text{cl}}}{\partial \dot{q}_k} = \frac{\partial W}{\partial q_k} = \dot{q}_k. \quad (2.10)$$

Here again, one can introduce the parities into Eq. (2.9) as

$$\frac{1}{2} \sum_k \left[\frac{1}{\sigma_k} \frac{\partial L}{\partial \dot{q}_k} \right]^2 + V(\vec{q}) = \frac{1}{2} \sum_k \left[\frac{\partial L}{\partial \dot{q}_k} \right]^2 + V(\vec{q}) = E, \quad (2.11)$$

where we have distinguished L from L_{cl} , since we may be already out of the bounds of Newtonian mechanics. Comparison of Eqs. (2.9) and (2.11) suggests a dynamical relation

$$\dot{q}_k = \frac{1}{\sigma_k} \frac{\partial L}{\partial \dot{q}_k}. \quad (2.12)$$

If $\sigma_k = 1$ for all k , this is nothing but Newtonian mechanics. However, we show below that a consistent theory of mechanics can be constructed also for general sets of $\{\sigma\} = \{\sigma_1, \sigma_2, \dots\}$.

First of all, define a real-valued parameter θ that mimics the role of time. (Note again that we are thinking of the time-independent HJ equation, and thus no physical time is involved here.) The dynamics is evolved along θ . Each coordinate has its own chronological parameter such that

$$\tau_k = \frac{\theta}{\sqrt{\sigma_k}}. \quad (2.13)$$

Next we regard the relation given in Eq. (2.12) as the redefinition of a Lagrangian $L(q, \dot{q}, \theta)$ for nonclassical motion,

$$\dot{q}_k = \frac{dq_k(\theta)}{d\theta} = \frac{1}{\sigma_k} \frac{\partial L(q, \dot{q}, \theta)}{\partial \dot{q}_k}, \quad (2.14)$$

the explicit form of which will be constructed later. The corresponding momentum is defined, on the other hand, by

$$p_k = \frac{dq_k(\theta)}{d\tau_k} = \sqrt{\sigma_k} \dot{q}_k, \quad (2.15)$$

which is purely imaginary for the anti-Newtonian motion. The reason for this definition will become clear later. A real-valued quasimomentum is defined by

$$\bar{p}_k = \frac{1}{\sqrt{\sigma_k}} p_k = \frac{1}{\sigma_k} \frac{\partial L(q, \dot{q}, \theta)}{\partial \dot{q}_k}, \quad (2.16)$$

which is essentially equivalent to \dot{q}_k . \bar{p}_k will be utilized in practical calculation, whereas p_k has only theoretical significance to facilitate investigation of, for example, symmetry properties in differential forms (see Sec. II D).

The equation of motion can be derived as usual in terms of the Euler-Lagrange variational principle,

$$\delta \int_{\theta_1}^{\theta_2} L(q, \dot{q}, \theta) d\theta = 0, \quad (2.17)$$

which is immediately followed by

$$\frac{d}{d\theta} \left[\frac{\partial L}{\partial \dot{q}_k} \right] - \frac{\partial L}{\partial q_k} = 0, \tag{2.18}$$

that is,

$$\sigma_k \dot{\bar{p}}_k = \sigma_k \frac{d\bar{p}_k}{d\theta} = \frac{\partial L}{\partial q_k}. \tag{2.19}$$

On the other hand, since we have the total derivative of the Lagrangian as

$$d \left[L - \sum_k \sigma_k \bar{p}_k \dot{q}_k \right] = \sum_k \sigma_k (\dot{\bar{p}}_k dq_k - \dot{q}_k d\bar{p}_k), \tag{2.20}$$

a Hamiltonian $H(\{\sigma\})$ can be introduced as usual by putting

$$dH(\{\sigma\}) = - \sum_k \sigma_k (\dot{\bar{p}}_k dq_k - \dot{q}_k d\bar{p}_k) \tag{2.21}$$

and hence

$$H(\{\sigma\}) + L = \sum_k \sigma_k \bar{p}_k \dot{q}_k. \tag{2.22}$$

Equation (2.21) leads to a new set of canonical equations of motion for a nonclassical motion as

$$\begin{aligned} \sigma_k \dot{\bar{p}}_k &= - \frac{\partial H(\{\sigma\})}{\partial q_k}, \\ \sigma_k \dot{q}_k &= \frac{\partial H(\{\sigma\})}{\partial \bar{p}_k}, \end{aligned} \tag{2.23}$$

from which the explicit form of the Hamiltonian can be obtained as

$$H(\{\sigma\}) = \sum_k \frac{\sigma_k}{2} \bar{p}_k^2 + V(\vec{q}). \tag{2.24}$$

The corresponding Lagrangian is also written down explicitly with use of the relation of Eq. (2.22). In these equations up to Eq. (2.24), the Hamiltonian has been

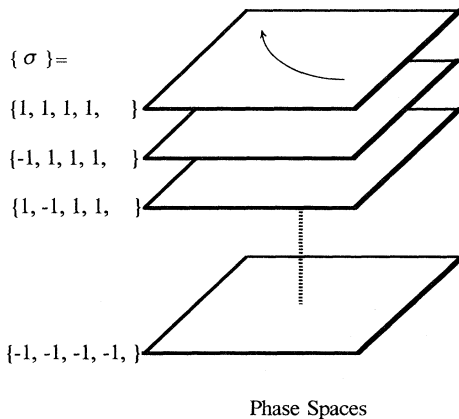


FIG. 1. The layer structure of the solution space of the Hamilton-Jacobi equation classified by the parity sets. The top and bottom sheets are, respectively, for Newtonian mechanics and instanton paths.

denoted by $H(\{\sigma\})$ in order to remind the reader that it is not the same as the standard Hamiltonian of Eq. (2.2). In what follows, we shall simply write it as H , unless confusion is expected otherwise.

Judging from the equations of Eq. (2.23), it would be almost appropriate to regard the role of the parities as

$$\sigma_k = \begin{cases} 1 & \text{for classical (Newtonian) motion} \\ -1 & \text{for nonclassical (anti-Newtonian) motion.} \end{cases}$$

However, it should be noted that these motions are generally coupled among different coordinates in a nonseparable system. Also, it is clear from the foregoing derivation that any local separability has not been applied.

The above equations of motion hold for an individual set of parities $\{\sigma_1, \sigma_2, \dots\}$, and thus all the trajectories generated in each set constitute a sheet, which in turn leads to a layer structure in the entire solution space, which is depicted in Fig. 1. We have two extreme sheets here, one being located at the top with all the parity positive, while the other is at the bottom having all negative parities. The former is trivially assigned to the ordinary Newton mechanics. In the latter is also obvious that the paths there are the so-called instanton paths [11(b),13].

Further, it is quite easy to show

$$\frac{dH}{d\theta} = 0. \tag{2.25}$$

So the Hamiltonian still bears the physical meaning of energy, and the energy is conserved along a path.

C. The principle of least action

The mechanics thus generalized leads us to a natural definition of an action integral such that

$$W_{cl} = \sum_k \int \sigma_k \bar{p}_k dq_k. \tag{2.26}$$

This real-valued integral is to be taken along a path generated by Eq. (2.23) within a given sheet. Since we will introduce another action integral in the next section, we shall call W_{cl} the path action.

As is checked easily, W_{cl} is not a solution of the HJ equation, unless all the parities happen to be positive unity. Nonetheless, the path action is theoretically important, since it satisfies the principle of least action just as in Newtonian mechanics, and is thus responsible for generating both classical and nonclassical paths. The proof for the principle of least action proceeds with almost complete parallelism with that for standard analytic mechanics [14]. We take a variation of

$$W_{cl} = \sum_k \int_{\theta_1}^{\theta_2} \sigma_k \bar{p}_k \dot{q}_k d\theta = \int_{\theta_1}^{\theta_2} (L + H) d\theta \tag{2.27}$$

such that

$$\Delta W_{cl} = \Delta \int_{\theta_1}^{\theta_2} L d\theta + E(\Delta\theta_2 - \Delta\theta_1), \tag{2.28}$$

where Δ requires the variation to be taken as a free-boundary problem, which should be compared to the variation δ in Eq. (2.17) under fixed boundary conditions

[14(a)]. After some lengthy manipulations, we reach

$$\Delta W_{\text{cl}} = \left[\left[-\sum_k \sigma_k \bar{p}_k \dot{q}_k + L + H \right] \Delta\theta \right]_{\theta_1}^{\theta_2} = 0, \quad (2.29)$$

which completes the proof. In the proof, the fundamental relations, namely, the energy conservation, Eq. (2.25), Lagrange's variational principle, Eq. (2.17), and the Hamiltonian-Lagrangian relation, Eq. (2.22), are all made use of.

D. Transformation property

The transformation property of the present mechanics has not yet been fully investigated. In order to see the invariance property inherent in the Hamilton system, the following coordinates are convenient:

$$\begin{aligned} Q_k &= \sqrt{\sigma_k} q_k, \\ P_k &= \sqrt{\sigma_k} \bar{p}_k = p_k, \end{aligned} \quad (2.30)$$

where both Q_k and P_k are purely imaginary, if $\sigma_k = -1$. Then Eq. (2.23) is transformed to

$$\begin{aligned} \dot{P}_k &= -\frac{\partial H(\{\sigma\})}{\partial Q_k}, \\ \dot{Q}_k &= \frac{\partial H(\{\sigma\})}{\partial P_k}, \end{aligned} \quad (2.31)$$

which looks very similar to the Hamilton canonical equations, and thereby rationalizes the definition of the momentum in Eq. (2.15). The proof for the theorem of absolute invariance due to Poincaré-Cartan [14(c)] can be applied to our case, which claims that a flow in phase space induced by the Hamiltonian $H(\{\sigma\})$ should conserve a two-form

$$\omega^2 = \sum_{k=1}^N dP_k \wedge dQ_k \quad (2.32)$$

and the higher-order differential forms analogous to this. The Stokes theorem [14] brings Eq. (2.32) back to the expression of the path action, Eq. (2.26). The integrability of nonclassical trajectories can be studied on the basis of Eqs. (2.26) and (2.32).

An important consequence from Eq. (2.32) is the Liouville theorem. The conservation of phase-space volume is thus assured in each sheet. Note again that the two-form in Eq. (2.32) is real valued irrespective of the parities. However, the volume conservation should not be confused with rapid (exponential) diminishing of the amplitude of a tunneling wave function, which is relevant to tunnel probability. This is our subject in the next section.

III. TWO KINDS OF ACTION INTEGRALS

A. An action integral as a solution to the HJ equation

As noted above, the path action Eq. (2.26) is not a solution of the time-independent HJ equation, once any one of the parities is set negative. This situation is markedly different from the basic idea due to Jacobi that an action integral satisfying the HJ equation should give rise to a

trajectory as its characteristic line [14]. This idea does not hold here. To be more precise, an action integral that satisfies the HJ equation can be different from the path action W_{cl} in the nonclassical domain.

In fact, once a path is obtained, a solution to the HJ equation (W_{HJ}), which is called the HJ action, can be readily constructed in such a way that

$$W_{\text{HJ}} = \sum_k \int \sqrt{\sigma_k} \bar{p}_k dq_k. \quad (3.1)$$

Again this integral is to be taken along the path. With the help of the usual relation [cf. Eq. (2.16)]

$$\frac{\partial W_{\text{HJ}}}{\partial q_k} = \sqrt{\sigma_k} \bar{p}_k = p_k \quad (3.2)$$

and the Hamiltonian of Eq. (2.24), the proof for W_{HJ} to satisfy the HJ equation is straightforward. Note also that not only W_{HJ} of Eq. (3.1) but also other functions such as

$$W = \sum_k \int \sigma_k \sqrt{\sigma_k} \bar{p}_k dq_k \quad (3.3)$$

can be a solution as well, since the latter is simply the complex conjugate of Eq. (3.1). It is quite straightforward to see that only in Newtonian mechanics does W_{HJ} coincide with W_{cl} .

Unlike W_{cl} , W_{HJ} can become complex, the imaginary part of it coming from the coordinates of negative parities. By writing

$$W_{\text{HJ}} = W_R + iW_I \quad (3.4)$$

the HJ equation is split into

$$\frac{1}{2} \sum_k \left\{ \left[\frac{\partial W_R}{\partial q_k} \right]^2 - \left[\frac{\partial W_I}{\partial q_k} \right]^2 \right\} + V(\vec{q}) = E \quad (3.5)$$

and

$$\vec{\nabla} W_R \cdot \vec{\nabla} W_I = 0. \quad (3.6)$$

These two relations have to be satisfied by any solution of the HJ equation, and they are in fact satisfied by W_{HJ} . The second equation is fulfilled because the coordinates with positive and negative parities are chosen to be orthogonal to each other.

B. Tunneling probability

A semiclassical wave function can be generally written as [11]

$$\psi = A \exp \left[\frac{i}{\hbar} W_{\text{HJ}} \right]. \quad (3.7)$$

The preexponential factor A need not be explicit here [11]. Inserting Eq. (3.4) into Eq. (3.7), one gets

$$\psi = A \exp \left[-\frac{1}{\hbar} W_I \right] \exp \left[\frac{i}{\hbar} W_R \right], \quad (3.8)$$

where the phase convention for W_{HJ} is taken so that W_I becomes positive. The first exponential term represents

the decrease of the norm of the wave function in a non-classical region.

In the classical limit, that is, $\hbar \rightarrow 0$, the wave function in Eq. (3.8) becomes obviously zero for any nonzero value of W_I , and thus we observe no tunneling practically. Accordingly, in macroscopic situation one can by no means realize the sheets other than the Newtonian one. However, as soon as one enters into microscopic physics, the non-Newtonian parts must be considered.

C. Connection problem

The Hamilton-Jacobi equation has in general multivalued solutions. As long as a set of parities is fixed, any path generated by Eq. (2.23) remains in the same sheet, and each sheet defines an independent branch of solutions. Tunneling solutions are hence obtained by connecting a nonclassical sheet with the classical one smoothly. In other words, tunneling begins when a classical path of $\{\sigma\} = \{1, 1, 1, \dots\}$ is connected at a point by changing one or more parities. After residing in tunneling sheet(s) for a while it comes back to a classical path at another point by returning to $\{\sigma\} = \{1, 1, 1, \dots\}$, and tunneling is over. From the viewpoint of the Hamilton-Jacobi theory alone, any complicated transition among sheets is equally accepted as long as the connections can take place smoothly. However, as a path stays in a tunneling region for a longer time, or more precisely larger θ , the survival probability of a tunneling wave function becomes exponentially smaller, as is suggested in Eq. (3.8). This is more likely so when the number of negative parities is larger.

At a point on a path where some of the parities are changed, the HJ actions have to be connected smoothly as well as the geometry of the path. In addition, the HJ equation (2.1) and the energy conservation law Eq. (2.25) require energy to be conserved globally through the connected paths. All these arguments suggest that a path should have zero momentum in a direction in which a parity is changed. Generally speaking, a coordinate normal to a caustic surface in configuration (q) space, is accepted as such a direction [1]. Suppose that a trajectory encounters a caustic point with no degeneracy. An orthogonal transformation of the coordinate system is performed so that the coordinate normal to the caustic surface is given a negative parity. For all the other (orthogonal) directions, the momenta and parities remain unchanged. Hence the trajectory enters a sheet to which a single negative parity is assigned. We therefore note that a different direction normal to a caustic surface gives rise to a different way of assignment of the parity set, even though the number of negative parities is the same.

Caustics are generally defined in a classical region with a Jacobian determinant in such a way that [11]

$$\det \left| \frac{\partial \vec{q}_f}{\partial \vec{p}_i} \right| = 0, \quad (3.9)$$

where $\vec{p}_i = \{p_1, p_2, p_3, \dots\}$ and \vec{q}_f are a momentum vector at the initial point and a position vector at the final end of a trajectory, respectively. The inverse of the Jacobian determinant is known to represent the density of

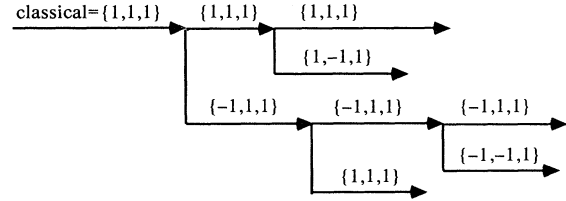


FIG. 2. Bifurcation of paths by changing the parities of motion.

paths in configuration space [11]. Caustics are important not only from the geometrical requirements, but because the amplitude of a wave function, the factor A in Eq. (3.7), becomes large (in fact, infinite in the primitive WKB function) at caustics, since A is essentially proportional to the square root inverse of the Jacobian determinant [11]. The calculation of caustics and coordinate transformation for any set of parities is defined in an analogous manner. The initial vector \vec{p}_i in Eq. (3.9) should be replaced with a quasimomentum $\vec{p}_i = \{\bar{p}_1, \bar{p}_2, \bar{p}_3, \dots\}$. The computation of the Jacobian determinant can be carried out with a straightforward extension.

A trajectory can bifurcate occasionally by switching its parities. In Fig. 2 is shown a schematic diagram of the proliferation of many bifurcations from a trajectory in a three-dimensional (3D) system. Suppose first that we have a classical trajectory with a parity set $\{1, 1, 1\}$ for $\{x, y, z\}$ coordinates, respectively. At a caustic point, this path can bifurcate into two trajectories; one continues to be classical. A nonclassical path is also generated by setting a new set, for instance $\{-1, 1, 1\}$, after an orthogonal transformation of the coordinates according to the geometry of the caustic surface. Hence it should be understood that the sets of parities in Fig. 2 are not necessarily assigned to the same coordinates $\{x, y, z\}$. The path thus having entered into a tunneling region can change its parities at another point and it either gets out of the tunneling region, enters different tunneling regions, or remains in the same tunneling sheet. In this way, infinitely many series of bifurcation can continue. Incidentally, the number of zero eigenvalues in Eq. (3.9) is not necessarily 1 at a caustic point, although this degeneracy is a minor case in general. Should it happen, some of the corresponding parities can be changed simultaneously. However, note that the number of parities to be changed can be smaller than the order of degeneracy. Therefore a path at this point can bifurcate into a number of paths. This aspect will be discussed in great detail in our forthcoming presentation [19].

Mathematically one can enjoy many varieties of bifurcations of nonclassical trajectories. But most of them are of little physical relevance because their quantum-mechanical amplitudes can be very small due to Eq. (3.8). In particular, a trajectory bearing more negative parities tends to have a smaller contribution. So does a trajectory staying longer in a nonclassical region. Thus trajectories that are physically significant are to be selected on this principle. More will be described in the presentation of the following numerical examples.

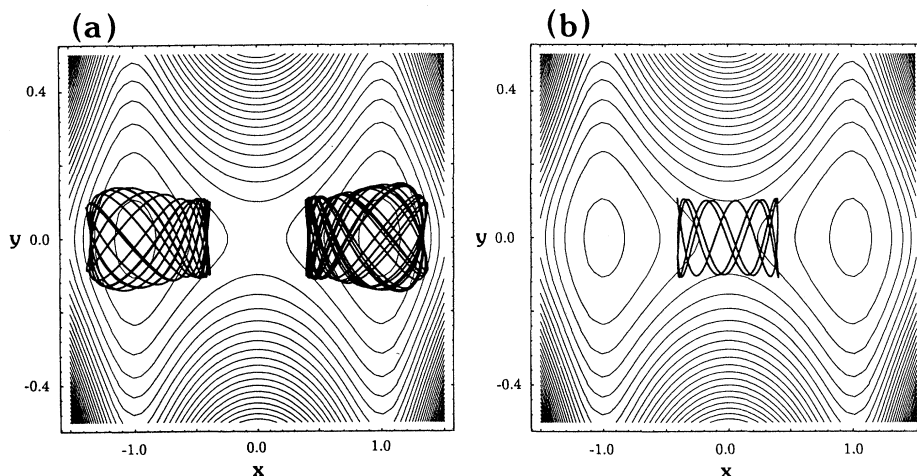


FIG. 3. (a) Two-dimensional double-well potential and two classical trajectories running on its classically allowed valleys. The trajectory begins from the bottom of the right valley, and ends up by moving out to the left valley after tunneling. (b) A tunneling path connecting the two trajectories.

IV. NUMERICAL EXAMPLES OF TUNNELING PATHS

In order to see what kinds of tunneling paths are generated, we present three numerical examples in this section. Basically, all the numerical calculations shown below have been done on a common basis: For a given potential function in an N -dimensional ($N \geq 2$) system, a classical trajectory is started with positive parities only. Along a path, caustics are found through the direct calculation of Eq. (3.9). The geometry of each caustic surface determines an orthogonal transformation of the coordinates, which in turn is used to assign a new set of parities. A new trajectory resumes running after some of the parities are turned to be negative with the same momenta as before. In particular, a zero component of the momentum should be assigned to the direction of the negative parity. Hence the trajectory is smoothly bifurcated. Then the newly created tunneling path runs for a while in the new coordinates until it hits another conjugate point. There, a similar procedure is repeated to let the path return into the classical region.

The tunneling probability depends dramatically on the magnitude of the Planck constant in a semiclassical situation. However, since we have no reason to choose a particular magnitude of \hbar in our adopted models, no results of tunneling probability will be reported, although we have carried out the computations.

2D double-well potential

The first example is a rather simple Hamiltonian system having a widely known potential called the squeezed double well [13(b)], that is,

$$H = \frac{p_x^2}{2m_x} + \frac{p_y^2}{2m_y} + \frac{1}{8}(x-1)^2(x+1)^2 + \frac{1}{2}[2.25 + 5(x^2-1)^2]y^2, \quad (4.1)$$

where $m_x = m_y = 1.0$ [20]. The potential surface is drawn

in Fig. 3. The squeezed double well is one of the potential functions for which Auerbach and Kivelson extensively studied two-dimensional potential tunneling in terms of the instanton paths with their path decomposition expansion [13]. This pioneering work has also treated the amplitude factor in their adiabatic fluctuation approximation [13(b)]. Our main aim in the present paper,

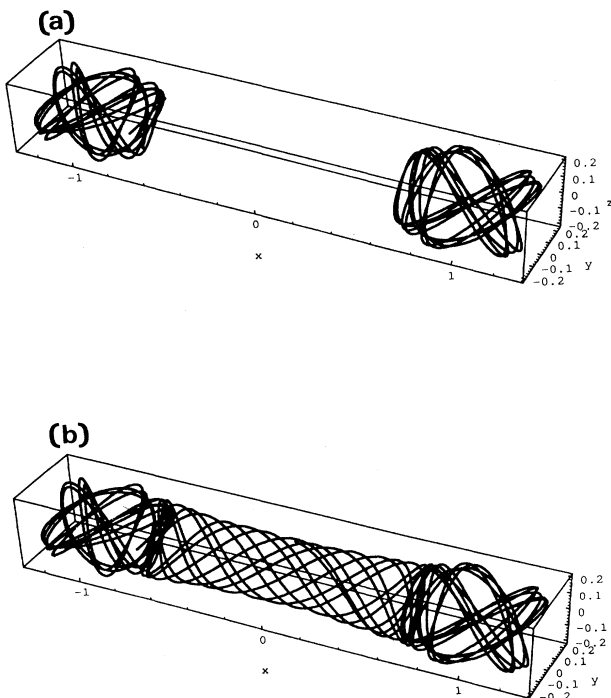


FIG. 4. (a) Two classical trajectories similar to those of Fig. 3(a), except that the potential is replaced with a 3D double-well function. (b) A tunneling path tying up the classical trajectories.

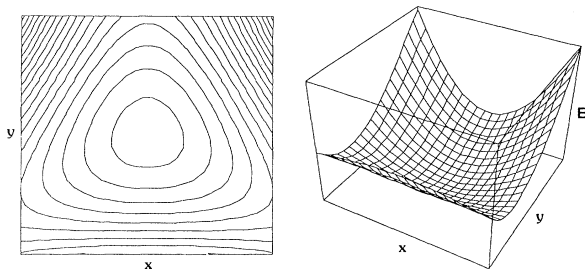


FIG. 5. The basin area of the Hénon-Heiles potential. There is no potential barrier in the angular direction.

on the other hand, is to show tunneling trajectories that are not instanton paths.

A trivial example of a turning point can be found on the straight line $y=0$, namely, the x axis. Changing the two parities into negative unity, an instanton path is generated [13(b)]. But our interest here is not in such a case. A trajectory in the right valley of Fig. 3(a) has the energy $E=0.12$, which is to be compared with the energy at the saddle point $E=0.125$. Thus this is simply a potential tunneling. The trajectory encounters a caustic point at the leftmost part, as is visibly confirmed. There, only the parity of the x direction is changed to be negative, and the trajectory enters into a tunneling region. No coordinate transformation is required in the present case. The trajectory in Fig. 3(b) represents the tunneling. In order to emphasize what the tunneling path looks like, we intentionally let it proceed without changing the parity at the first caustic point, which is seen in the leftmost point in the figure. This is, of course, an extremely unfavorable procedure that should result in a very small tunneling probability. At an instance when the tunneling trajectory comes to the third caustic point, which is again seen at the leftmost part, the negative parity has been brought back to be positive, and a trajectory comes out in the left-side valley as a purely classical path. This is seen as the trajectory in the left-hand-side valley of Fig. 3(a).

3D double-well potential

The next system is a straightforward extension of the above example to a three-dimensional system as

$$H = \frac{p_x^2}{2m_x} + \frac{p_y^2}{2m_y} + \frac{p_z^2}{2m_z} + \frac{1}{8}(x-1)^2(x+1)^2 + \frac{1}{2}[2.25 + 5(x^2-1)^2]y^2 + \frac{1}{2}[2.25 + 5(x^2-1)^2]z^2 \tag{4.2}$$

with $m_x = m_x = 1.0$ and $m_z = 1.0087$. The masses are chosen so as to break the symmetry for the reason of graphic presentation. The energy of the trajectory under study is $E=0.108$, and again the saddle point is as high as $E=0.125$. Two purely classical trajectories in Fig. 4(a) are in two symmetrical valleys which are separated by a saddle, the right one being the starting trajectory. At a caustic point along this trajectory, a tunneling path is created as shown in Fig. 4(b). As in the 2D case above, the tunneling trajectory has only one negative parity in the x direction, and again the three-way trip has been enforced for the presentation. At the caustic point in this tunneling path, all the parities are brought back to positive values, and a classical trajectory in the left valley of Fig. 4(a) comes about. This example verifies that the theory can be easily applied to as large a system as the ordinary classical trajectory method can produce. Nonetheless, to our best knowledge, we are aware of no other calculation for 3D tunneling of noninstanton type by means of the other methods.

Dynamical tunneling in Hénon-Heiles system

We consider dynamical tunneling in the well-known Hamiltonian system due to Hénon and Heiles [21], that is,

$$H = \frac{p_x^2}{2m_x} + \frac{p_y^2}{2m_y} + \frac{1}{2}(x^2 + y^2) + x^2y - \frac{1}{3}y^3 \tag{4.3}$$

To make the dynamics a little simpler by breaking symmetry, we take the masses as $m_x = 1.0087$ and $m_y = 1.0$.

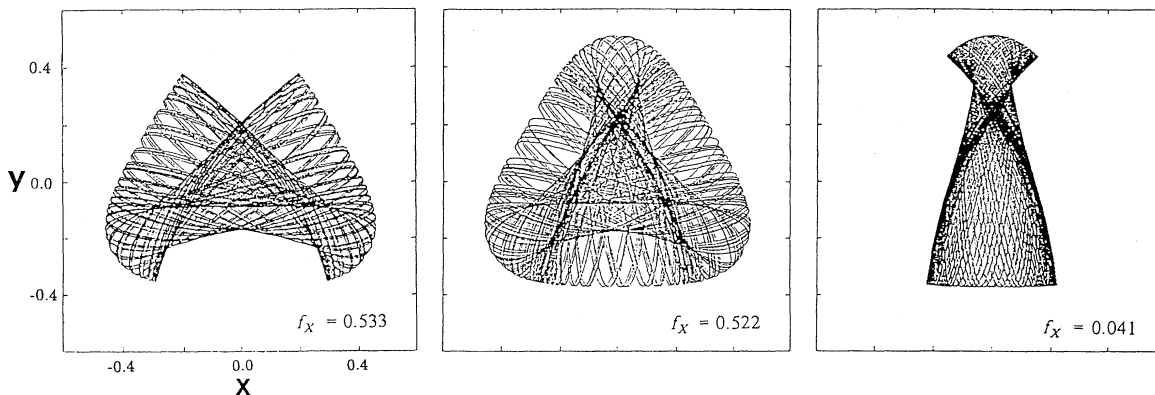


FIG. 6. Some of the typical modes in the Hénon-Heiles system. All these have the same energy $E=0.09$ and different initial conditions labeled with f_x .

The potential has a basin around the origin which can bound trajectories of energy less than $\frac{1}{6}$. The contour plot and the perspective view mainly of the basin area are drawn in Fig. 5. On the other hand, no trajectory is trapped outside the basin. The most significant feature of the potential is that the basin area does not have potential barrier in the angular direction around the origin. Nevertheless, the system bears several distinctive modes. A clear example is given in Fig. 6, in which all the trajectories share the same energy $E=0.09$, but have different initial conditions [9]. All the trajectories start from $x=y=0$ at the initial time with the positive momenta $p_x, p_y \geq 0$. The trajectories are labeled with f_x , which means the initial ratio of the energy assigned to the x coordinate to the total energy. Two different types of librations and rotations (leftward and rightward) are confirmed in Fig. 6. They are all supposed to wind around different tori.

Since the initial condition can be changed continuously with f_x , one can ask oneself what happens in between these clear-cut modes. For example, what is the mode of a trajectory of a parameter f_x in a very small interval $[0.522, 0.533]$ (see Fig. 6). This is actually a motion in a thin quasiseparatrix and is quite interesting. The motion first shows either libration (as in $f_x=0.533$) or left or right rotation (as in $f_x=0.522$) depending on f_x chosen. This mode is very clear at least macroscopically and can be identified numerically with a clear-cut quantity [9]. Then all of a sudden a transition from the mode to one of the other possible modes occurs. The transitions among the clear modes continue with no definite frequency [9]. This weakly chaotic mode defines a different kind of large-amplitude motion. We have studied the spectroscopic characterization of its quantum analog [10].

When a quantum state is localized mainly in a torus area rather than the thin quasiseparatrix, one can consider the possibility of tunneling among the available tori such as those described above, namely, dynamical tunneling. A classical trajectory of $f_x=0.533$ having a libra-

tion mode is considered here just as an example (see Fig. 6). It has many caustic points widely distributed in the configuration space, as is seen in Fig. 7(a). The outer caustics enveloping the trajectory in the region of large values of x^2+y^2 , where the potential energy becomes very close to the total energy, form systematic caustic lines. It has turned out that all the tunneling paths starting from this type of caustic go outside the basin without encountering a caustic point inside it. They eventually run away infinitely far from the origin, and hence do not give rise to dynamical tunneling. On the other hand, the caustics depicted in Fig. 7(b), which are extracted from those of Fig. 7(a), are actually associated with dynamical tunneling. A little more than 10% of the caustics examined are thus responsible for dynamical tunneling. This result suggests that the *chance* of tunneling would not be small. In our quantum-mechanical calculations, on the other hand, we have often observed that mixing of rotation and libration modes is so strong that they are not well separated [10], which should reflect frequent occurrence of tunneling.

Among the caustics in Fig. 7(b), we pick up a point located at $(x, y) = (-0.33, -0.10)$ [see Fig. 8(a) for the scale], and follow a tunneling path emanating from there. Since the caustic line has an angle about 13.8° measured counterclockwise from the positive x axis, the coordinates are rotated by the same angle clockwise to form, say, (x', y') coordinates, so that the zero-momentum component is directed towards the y' axis. The parity in this direction is changed to be negative unity and the tunneling path runs until the first caustic is encountered along this path [Fig. 8(b)]. At this point, namely, $(x', y') = (0.32, 0.09)$ [corresponding to $(x, y) = (0.29, 0.16)$], the (x', y') -coordinate system is rotated 30.4° anticlockwise to the (x'', y'') coordinates. Then the parities are brought back to $\{1, 1\}$. The new classical path thus resumed happens to be bound with the mode of left rotation in the basin [Fig. 8(c)].

We have also examined the instability of the tunneling

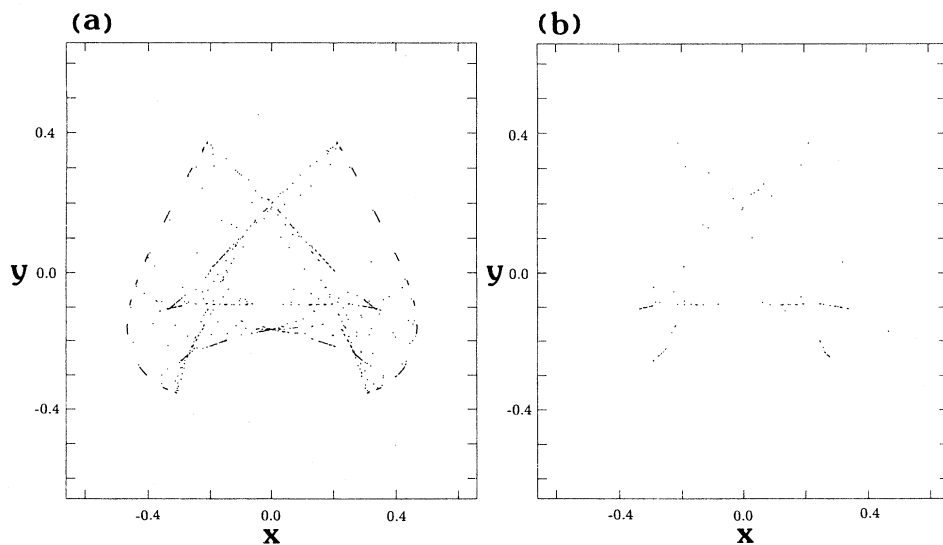


FIG. 7. (a) A set of the many caustic points lying on the trajectory of $f_x=0.533$ of Fig. 6. The longer run of the trajectory will generate more caustics. (b) Caustics giving rise to dynamical tunneling. The tunneling paths emanating from all the other caustics eventually run away from the basin area.

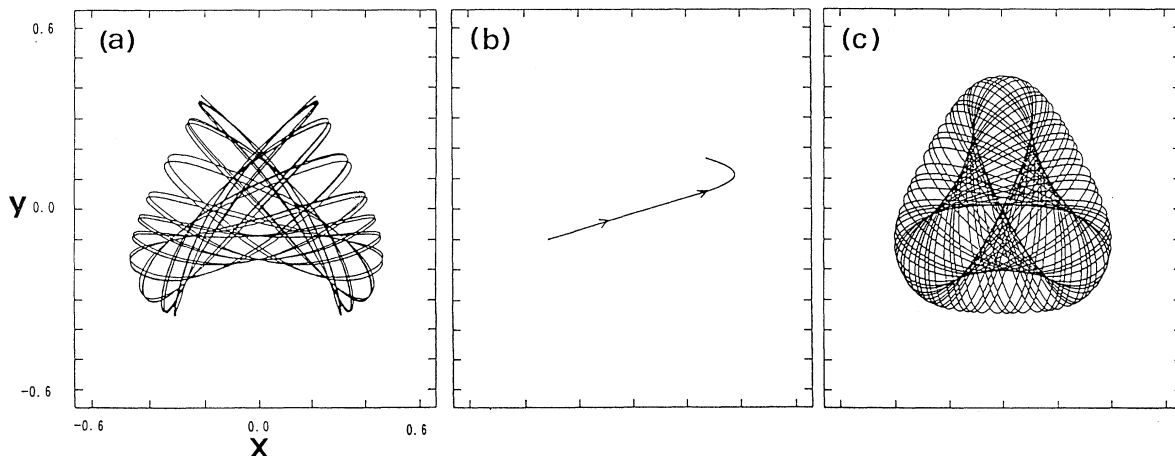


FIG. 8. An example of dynamical tunneling. (a) An initial classical path corresponding to $f_x=0.533$ in Fig. 6 encounters a caustic at $(x,y)=(-0.33,-0.10)$. (b) A tunneling path starts there and has its first caustic at $(x,y)=(0.29,0.16)$. (c) From this point is created the final classical path of left rotation.

path, since our system is weakly chaotic and the individual modes such as the libration and rotation modes are separated classically by chaotic zones. Chaos can be detected by looking at the eigenvalues of the Jacobian matrix [3-5]

$$\frac{\partial(\vec{q}_f, \vec{p}_f)}{\partial(\vec{q}_i, \vec{p}_i)}, \tag{4.4}$$

the minor of which has already appeared in Eq. (3.9).

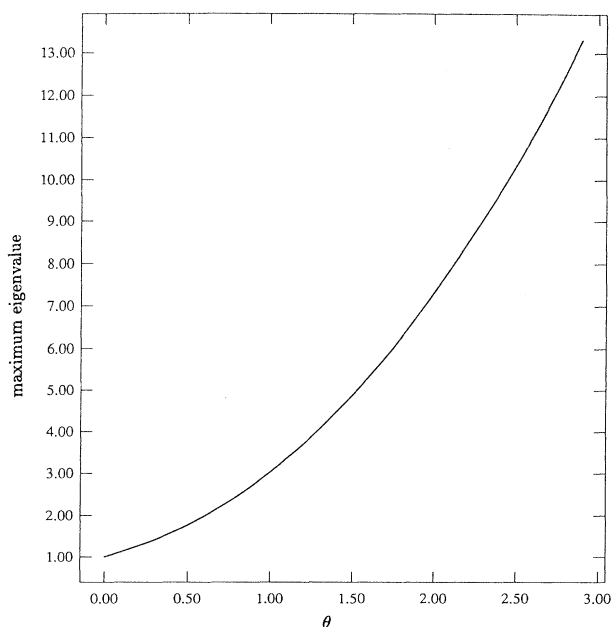


FIG. 9. The stability of the tunneling path of Fig. 8(b). The largest among the absolute values of the eigenvalues is plotted versus θ . The Liapunov exponent obtained from this curve is 0.888, and hence this tunneling path is considerably unstable.

Since our system is a two-dimensional Hamilton system, its eigenvalues should be obtained as a set $\{e^{ia}, e^{-ia}, e^{ib}, e^{-ib}\}$ [14]. A complex value a or b indicates (local) chaos, while if both are real the system is stable. Figure 9 displays the largest absolute magnitude among the eigenvalues as a function of the chronological parameter θ . As seen directly, this particular tunneling path is considerably unstable. In fact, the Liapunov exponent evaluated from this curve is 0.888. Although the role of chaos in tunneling probability is not yet clear, it can be conceived that a stable tunneling path should have a stable family of tunneling paths around it (with some finite measure) and hence contribute positively to the tunneling probability. In any case, the interplay between tunneling and chaos requires much study [19].

The second example is a path of dynamical tunneling from the same classical path as the first example of $f_x=0.533$ but starting from a different caustic point (Fig. 10). The tunneling path is rather more complicated here. It starts at a point $(0.09, -0.09)$, which is marked by A in Fig. 10(b). Only a slight rotation of the coordinates is required in this case. It proceeds rightward first, and happens to encounter a turning point at the point B . This particular point is not detected by the condition of Eq. (3.9) but by [11(b)]

$$\frac{\partial E(q_f, q_i, \theta)}{\partial \theta} = 0, \tag{4.5}$$

where $E(q_f, q_i, \theta)$ is the energy required for a path to travel from q_i to q_f during a given "time" θ . At this turning point, one can change two parities at the same time or one of the two parities, which can give rise to three new paths. This phenomenon is quite interesting and will be reported elsewhere. On this occasion, we do not consider this possibility. The path is simply bounced back without changing the parities there, and thus re-traces the same path to another caustic point C of $(-0.37, -0.16)$. There the tunneling is over and a new

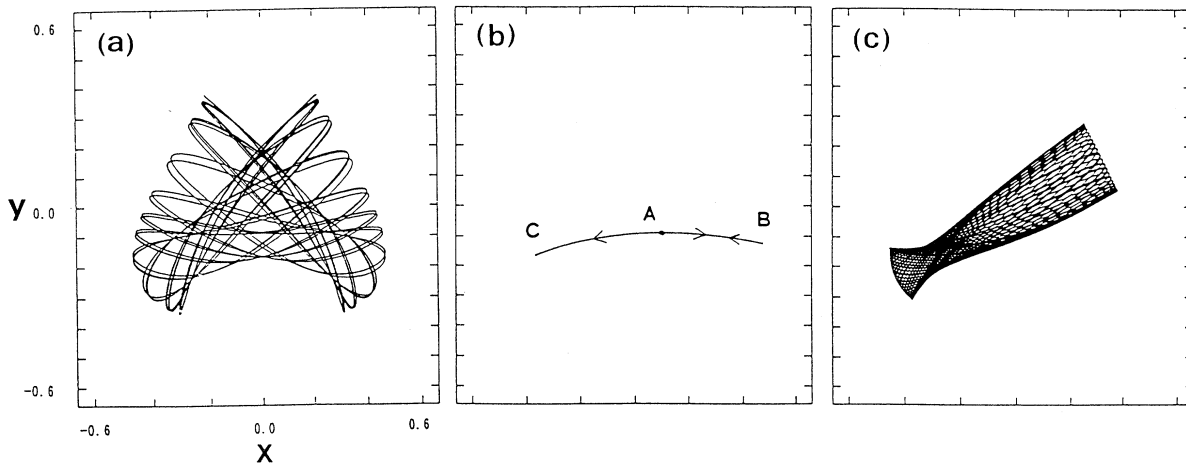


FIG. 10. The second example of dynamical tunneling from the same trajectory as that in Fig. 8. (a) Another caustic is found at point A (0.09, -0.09). (b) A tunnel path is generated at that point and proceeds to point B which is a turning point. It is forced to bounce back there without returning to the classical domain and reaches point C , which is a caustic point. There it comes back to the Newtonian sheet. (c) A new librational mode shows up there.

classical path is generated as shown in Fig. 10(c). Again, the tunneling path is chaotic, as shown in Fig. 11, and the Liapunov exponent is in fact 1.064.

V. CONCLUDING REMARKS

We have shown that complex solutions for the time-independent Hamilton-Jacobi equation can be propagated along newly constructed paths in real-valued configuration space. The paths are generated by introducing the parity set, and the entire space of all the possi-

ble solutions forms a layer structure composed of independent sheets, each of which defines a branch of solutions to be characterized by a parity set. Two extremes of the sheets are assigned to the ordinary Newton mechanics for which all the parities are positive unity, and to the space of instanton paths having all the parities negative. It has also been shown that equations of motion are associated with each sheet to evolve trajectories, and that two kinds of action integrals are integrated along a path. One is the path action, which is real and satisfies the principle of least action, but is not a solution of the HJ equation. The other, called the HJ action, can take a complex value and satisfies the Hamilton-Jacobi equation. These two actions happen to coincide with each other only in Newton mechanics.

These local solutions in the non-Newtonian sheets, for which at least one of the parities is negative, are of physical significance to represent tunneling only when they are considered in the semiclassical or quantum context. In particular, it is the HJ action that should be taken in the WKB wave function, the imaginary part of which represents the decay of a wave function in a tunneling region.

Some numerical examples have been presented. In particular, we have clearly shown dynamical tunneling between the distinctive modes in the Hénon-Heiles Hamiltonian. Since the chaotic nature of the tunneling trajectories leads to an interesting phenomenon, we will report more on this in our forthcoming presentation [19]. We have also calculated a tunneling path of noninstanton type in three-dimensional space for which only one direction bears a negative parity. This numerical calculation has demonstrated that the present theory can be applied to large systems in a straightforward manner. In a large system, only the instanton-type theory has been a practical method so far [13]. However, it is quite natural to expect that an instanton-type path, in which all the parities are set negative, would result in only an extremely small

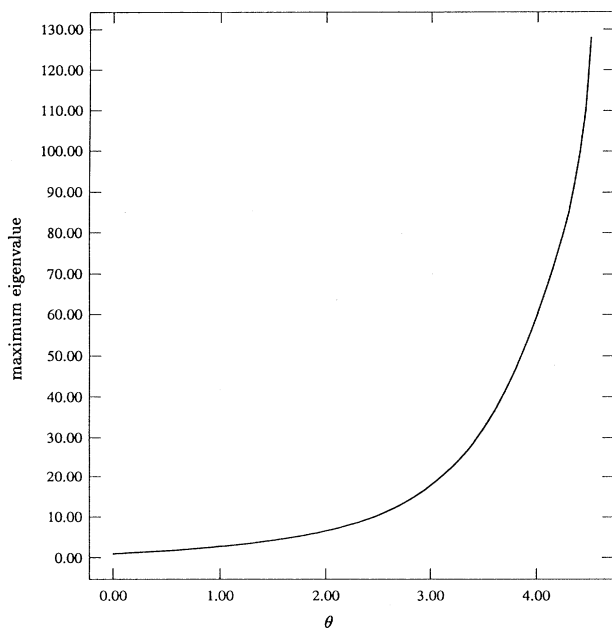


FIG. 11. The stability of the tunneling path of Fig. 10(b). The Liapunov exponent is 1.064. This is also unstable.

tunneling probability as the degrees of freedom increase. We will report the effect of high dimensionality on dynamical tunneling as well as tunneling in a curved space in our future presentation [19].

We have not described very precisely the connection problem of solutions in neighboring sheets. Takada and Nakamura gave an excellent theory for the multidimensional connection problem of global solutions of the time-independent HJ equation [2]. The connection problem is quite important to our scheme, too. However, since we have treated local solutions in the present paper, and since our theory can be readily extended to the time-

dependent Hamilton-Jacobi equation, this aspect will be reported with more examples of three- or higher-dimensional systems as well as tunneling in scattering problems [19].

ACKNOWLEDGMENTS

The authors thank N. Hashimoto and C. Seko for valuable discussions. This work has been supported in part by a Grant in Aid from the Ministry of Education, Science, and Culture of Japan.

-
- [1] Z. H. Huang, T. E. Feuchtwang, P. H. Culter, and E. Kaze, *Phys. Rev. A* **41**, 32 (1990).
- [2] S. Takada and H. Nakamura, *J. Chem. Phys.* **100**, 98 (1994), and references cited therein.
- [3] (a) A. J. Lichtenberg and M. A. Lieberman, *Regular and Stochastic Motion* (Springer, Berlin, 1983); (b) V. I. Arnold and A. Avez, *Ergodic Problems of Classical Mechanics* (Benjamin, Reading, MA, 1968).
- [4] (a) R. Z. Sagdeev, D. A. Usikov, and G. M. Zaslavsky, *Nonlinear Physics* (Harwood Academic, Chur, Switzerland, 1988); (b) M. Tabor, *Chaos and Integrability in Nonlinear Dynamics* (Wiley, New York, 1989); (c) *Chaos*, edited by D. K. Campbell (AIP, New York, 1990).
- [5] (a) A. M. Ozorio de Almeida, *Hamiltonian Systems: Chaos and Quantization* (Cambridge University Press, Cambridge, England, 1988); (b) M. C. Gutzwiller, *Chaos in Classical and Quantum Mechanics* (Springer, New York, 1990); (c) H. A. Cerdeira, R. Ramaswamy, M. C. Gutzwiller, and G. Casati, *Quantum Chaos* (World Scientific, Singapore, 1991).
- [6] (a) M. C. Gutzwiller, *J. Math. Phys.* **11**, 1791 (1970); **12**, 343 (1971); (b) R. B.alian and C. Bloch, *Ann. Phys. (N.Y.)* **60**, 401 (1970); **85**, 514 (1974); (c) K. Takatsuka, *Phys. Rev. A* **45**, 4326 (1992); *Prog. Theor. Phys.* **91**, 421 (1994), and references cited therein.
- [7] I. C. Percival, *Adv. Chem. Phys.* **36**, 1 (1977).
- [8] S. Tomsovic and E. J. Heller, *Phys. Rev. Lett.* **67**, 664 (1991); P. W. O'Connor, S. Tomsovic, and E. J. Heller, *Physica D* **55**, 340 (1991); M. A. Sepúlveda, S. Tomsovic, and E. J. Heller, *Phys. Rev. Lett.* **69**, 402 (1992); S. Tomsovic and E. J. Heller, *ibid.* **70**, 1405 (1993).
- [9] K. Takatsuka, *Chem. Phys. Lett.* **204**, 491 (1993); *Bull. Chem. Soc.* **66**, 3189 (1993).
- [10] N. Hashimoto and K. Takatsuka (unpublished).
- [11] As reviews of semiclassical theory, see (a) M. V. Berry and K. E. Mount, *Rep. Prog. Phys.* **35**, 315 (1972); (b) L. S. Schulman, *Techniques and Applications of Path Integration* (Wiley, New York, 1981); (c) V. P. Maslov and M. V. Fedoriuk, *Semiclassical Approximation in Quantum Mechanics* (Reidel, Dordrecht, 1981).
- [12] L. D. Landau and E. M. Lifshitz, *Quantum Mechanics* (Pergamon, New York, 1958).
- [13] (a) A. Auerbach, S. Kivelson, and D. Nicole, *Phys. Rev. Lett.* **53**, 411 (1984); (b) A. Auerbach and S. Kivelson, *Nucl. Phys.* **B257** [FS14], 799 (1985).
- [14] (a) H. Goldstein, *Classical Mechanics* (Addison-Wesley, Reading, MA, 1980); (b) E. T. Whittaker, *A Treatise on the Analytic Dynamics of Particles and Rigid Bodies*, 4th ed. (Cambridge University Press, Cambridge, England, 1959); (c) V. I. Arnold, *Mathematical Methods of Classical Mechanics* (Springer, Berlin, 1978); (d) R. Abraham and J. E. Marsden, *Foundation of Mechanics*, 2nd ed. (Addison-Wesley, Reading, MA, 1985).
- [15] See, for instance, W. Yourgrau and S. Mandelstam, *Variational Principles in Dynamics and Quantum Theory* (Dover, New York, 1979).
- [16] J. Knoll and R. Schaeffer, *Ann. Phys. (N.Y.)* **97**, 307 (1976).
- [17] M. Wilkinson, *Physica D* **21**, 341 (1986).
- [18] T. Banks, C. Bender, and T. T. Wu, *Phys. Rev. D* **8**, 3346 (1973); T. Banks and C. M. Bender, *ibid.* **8**, 3366 (1973).
- [19] H. Ushiyama and K. Takatsuka (unpublished).
- [20] The parameters used in Eq. (4.1) have been taken from Ref. [2].
- [21] M. Hénon and C. Heiles, *Astron. J.* **69**, 73 (1964).